Analysis of a Highly Nonlinear Lorentz Force Linear Motion Electromagnetic Actuator Using EMS

Ian Hunter, Ph.D. and Serge Lafontaine, Ph.D
Massachusetts, USA

Introduction

Linear motion electromagnetic actuators exploiting the Lorentz force are often used in applications requiring high bandwidth motion. A "loud speaker" or "voice-coil" actuator, as shown in Figure 1, is an example of such a device. Early computer hard disk drives used such Lorentz force linear motion actuators to move the magnetic recording heads radially over the spinning disks.
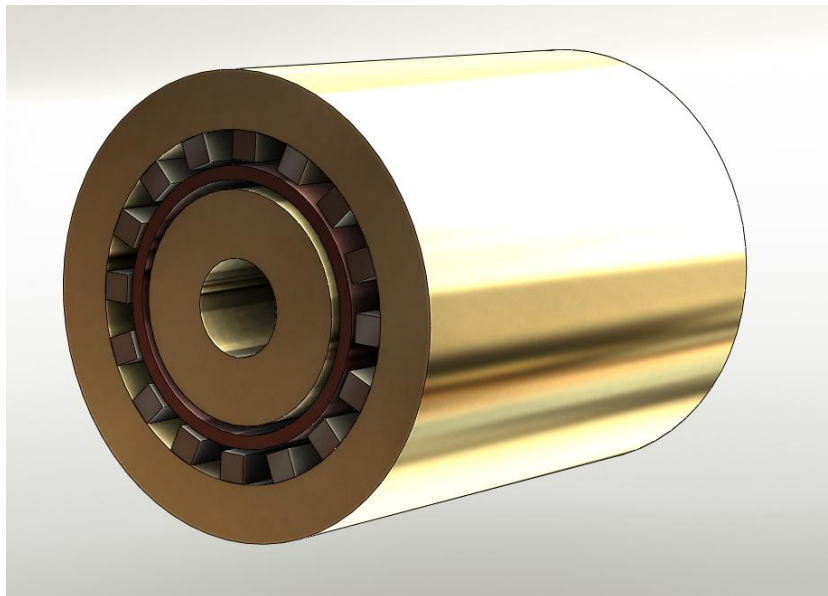

Figure 1. SolidWorks 9 CAD model of an electromagnetic actuator. The square bar magnets (silver) surround the copper coil. The inner and outer iron magnetic path is shown in gold. The copper coil is wound on a former (not shown) which slides on bearings (also not shown) mounted within the actuator.
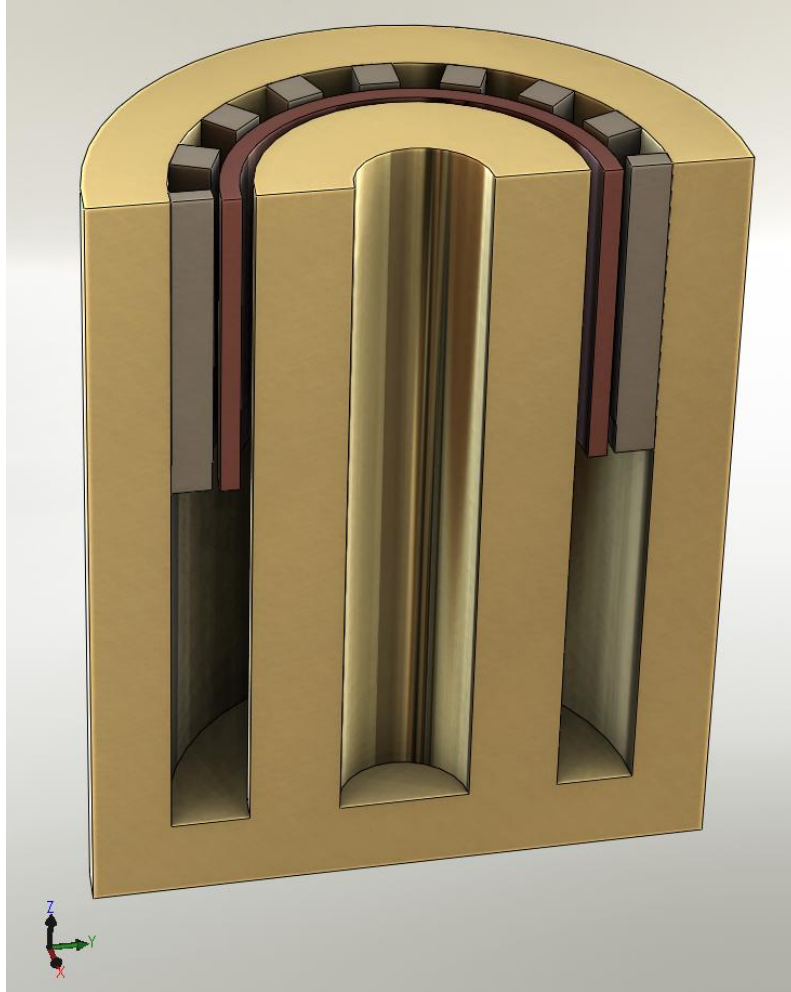
Figure 2. Cross-sectional slice through the middle of the actuator. Note that the coil (individual wires not shown) moves along the z-axis. The magnetic field runs radially from the magnets through the coil to the inner cylindrical magnetic return path.

Figure 2 shows the cross-section through a cylindrical Lorentz force linear motion actuator in which the static magnetic field is generated by magnets surrounding the coil. In this example the square section magnets are magnetized in the radial direction and the magnetic return path is provided by low carbon content steel (shown in gold in Figure 2). Note that the current flowing in the coil is orthogonal (at right angles) to the static magnetic field. The resulting Lorentz force is orientated in the third orthogonal axis. A simplistic analysis of this actuator predicts that the static force (Lorentz force), F (Newton, N), generated by the coil will be a linear function of the current, I (Amp, A), the number of turns, N, the length, L (meter, m) of coil exposed to the magnetic field (i.e. the coil circumference length here) and magnetic flux density, B (Telsa, T) passing through the coil generated by the magnets (alone).

$$F = I\,N\,L\,B \tag{1}$$

This equation is found to predict the coil force well in experiments when the coil current density is less than 10^6 A/m^2. Such current densities are rarely exceeded in audio system loud speakers. However in woofers (and in particular competition woofers) higher current densities will often arise. Current densities of above 10^8 A/m^2 are used in some higher performance devices. For example the linear electromagnetic actuator developed for use in the needle free drug delivery technology developed in the BioInstrumentation Laboratory at MIT uses coil current densities as high as 2×10^8 A/m^2 for short periods (Taberner et al., 2006; Wendell et al., 2006; Hemond, et al., 2006).

At these high current densities the effect of the magnetic field generated by the coil becomes significant and must be considered. In particular in the presence of any ferromagnetic material in the magnetic return path the coil generates a force which is different from the force predicted in the equation above. For example current in the coil shown above will still generate a force even when the magnets are completely removed from the actuator. In the following we will consider a "pull" force to be negative and a "push" force to be positive.

The actuator shown above was explicitly built to behave in a highly nonlinear fashion to test the ability of the electromagnetic finite element software, EMS, produced by ElectroMagnetic Works (Montréal, Canada) (www.electromagneticworks.com) to predict the actuator's current to force behavior. The magnets were spaced out to further complicate the actuator geometry as a further test of EMS.

In the following paper the current to force predictions of the EMS magnetostatic analysis are compared with those measured experimentally. As will be shown EMS accurately predicts the highly nonlinear current to force relation shown by this geometrically complex actuator. Normally such nonlinearities would be highly undesirable and would be avoided. Because EMS is able to account for these nonlinearities it may of course also be used to help create and validate designs in which the nonlinearities are minimized.

Experimental Apparatus

Two types of experimental apparatus were used. The first apparatus permits a wide range of both static and dynamic measurements to be made of the current to force relation of a linear motion actuator rigidly attached to a force sensor. In this apparatus the actuator coil is held in a fixed position (although this position may be changed). In the second apparatus the coil is attached to a movable load and so the coil is able to move against the load. This second apparatus also permits the coil to be clamped at fixed locations.
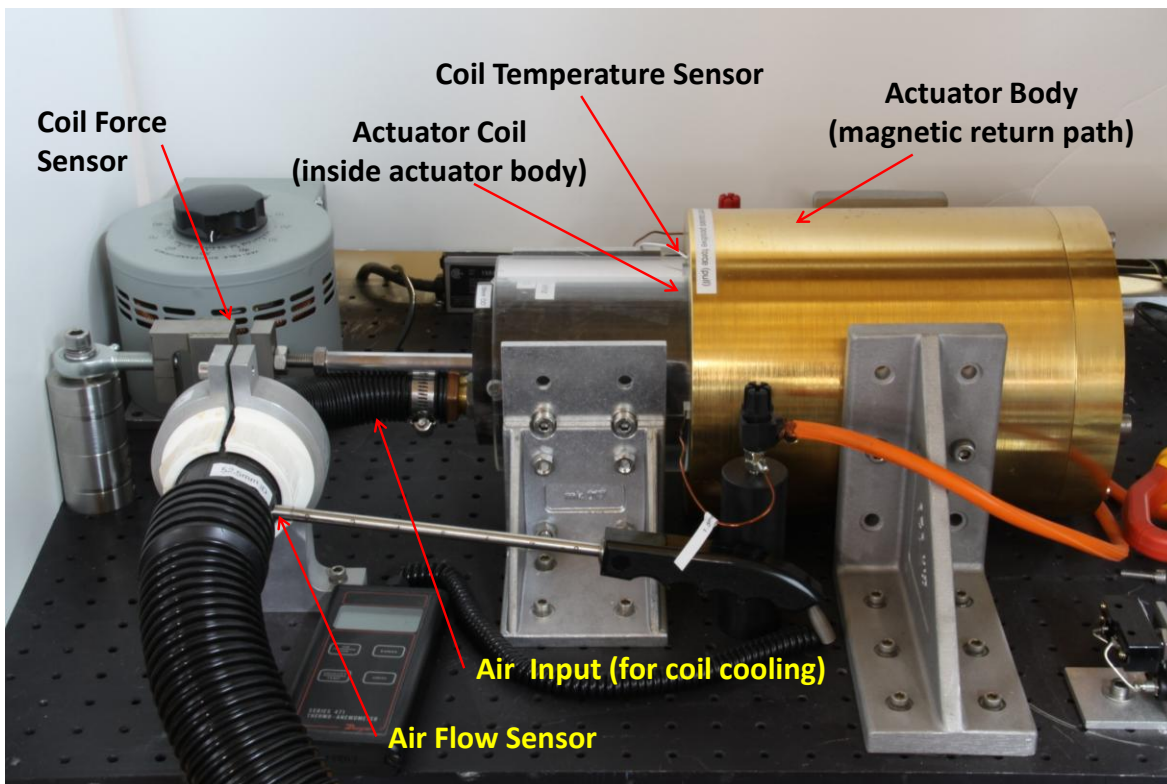
Figure 3. Apparatus used for linear actuator static and dynamic measurements with coil position fixed. A Hall effect sensor (not shown) is used to measure the magnetic flux density in the air gap separating the coil from the magnets.

Figure 3 shows the first apparatus. Notice that the coil is connected to a force sensor (s-beam strain gage load cell) which is in turn connected to a computer via strain gage conditioning electronics and a high resolution analog to digital converter. The temperature of the coil is measured with a platinum resistive sensor which is also connected to the computer. A Hall effect sensor placed in the air gap between the coil and the surrounding magnets is used to measure the magnetic flux density. The coil is cooled by pressurized air which flows over the coil. The air flow is generated by an air pump which may be set to a range of air flows. The flow

is measured by a hot wire anemometer sensor. The current delivered to the coil is computer controlled via a custom IGBT based power amplifier which is connected to a large battery bank. A wide range of static and dynamic positive and negative currents may be delivered to the coil. The coil current is measured by a Hall effect current sensor. The coil voltage is also measured by the computer.
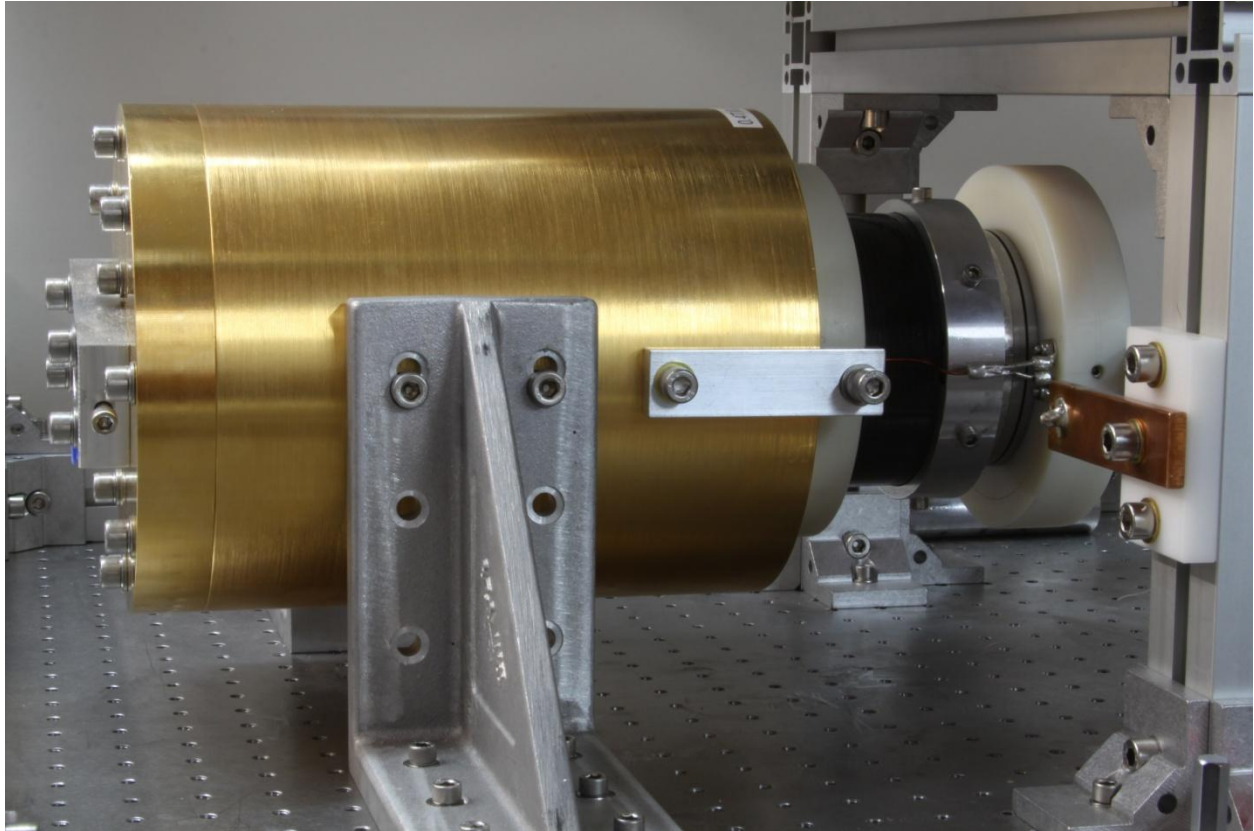
Figure 4. A linear actuator mounted in the second apparatus.

Figure 4 shows a linear actuator mounted in the second apparatus which is primarily used for testing the actuator characteristics during coil linear movement. However in the following analysis the coil was set in its mid position. In this position the 100 mm long coil is aligned with the 100 mm magnetic field (i.e. all parts of the coil are exposed to the static magnetic field generated by the magnets).

Experimental Results

Figure 5 shows an example of coil force (N), current (A), voltage (V) and magnetic flux density (T) recorded while a -50 A current pulse was applied to the coil (pulling).
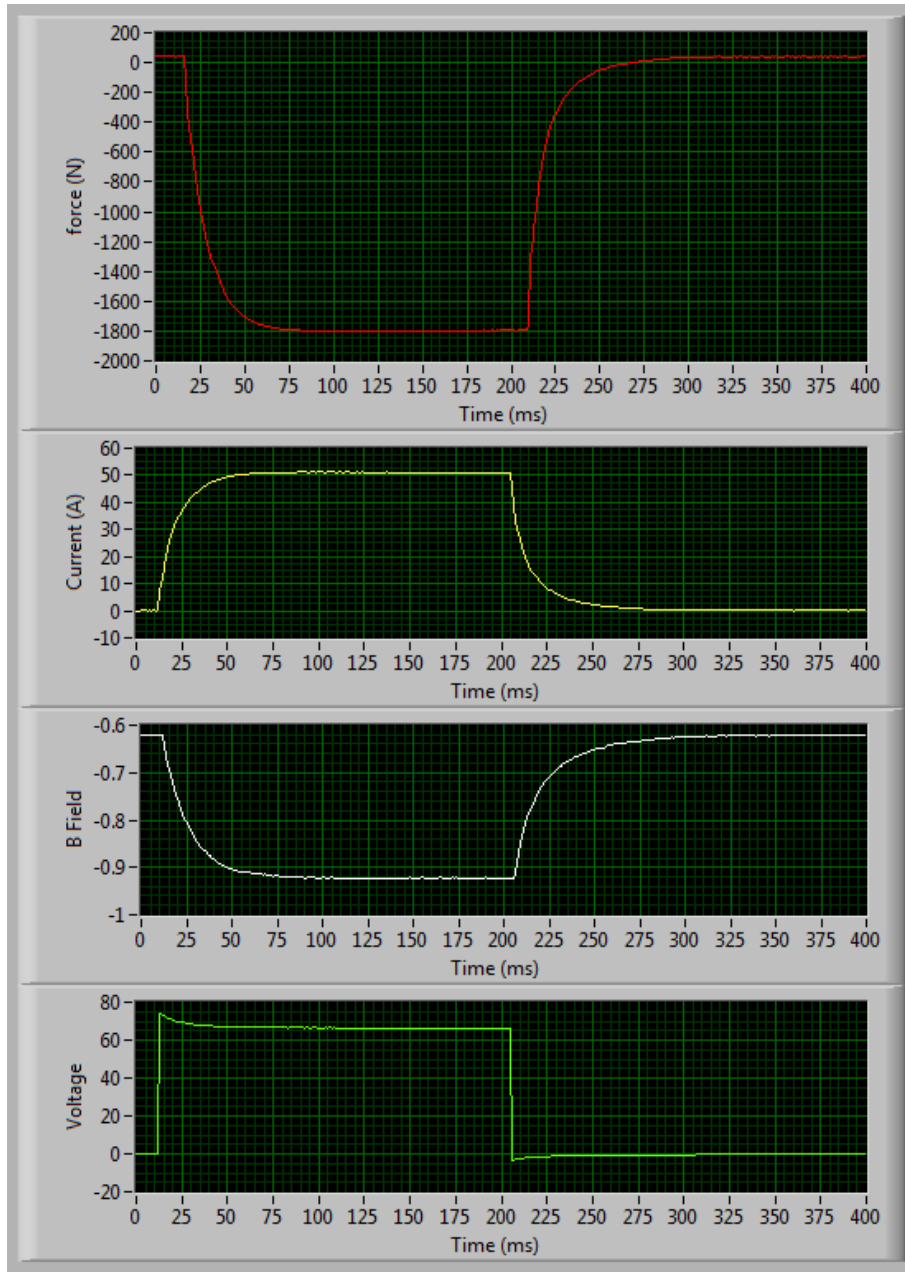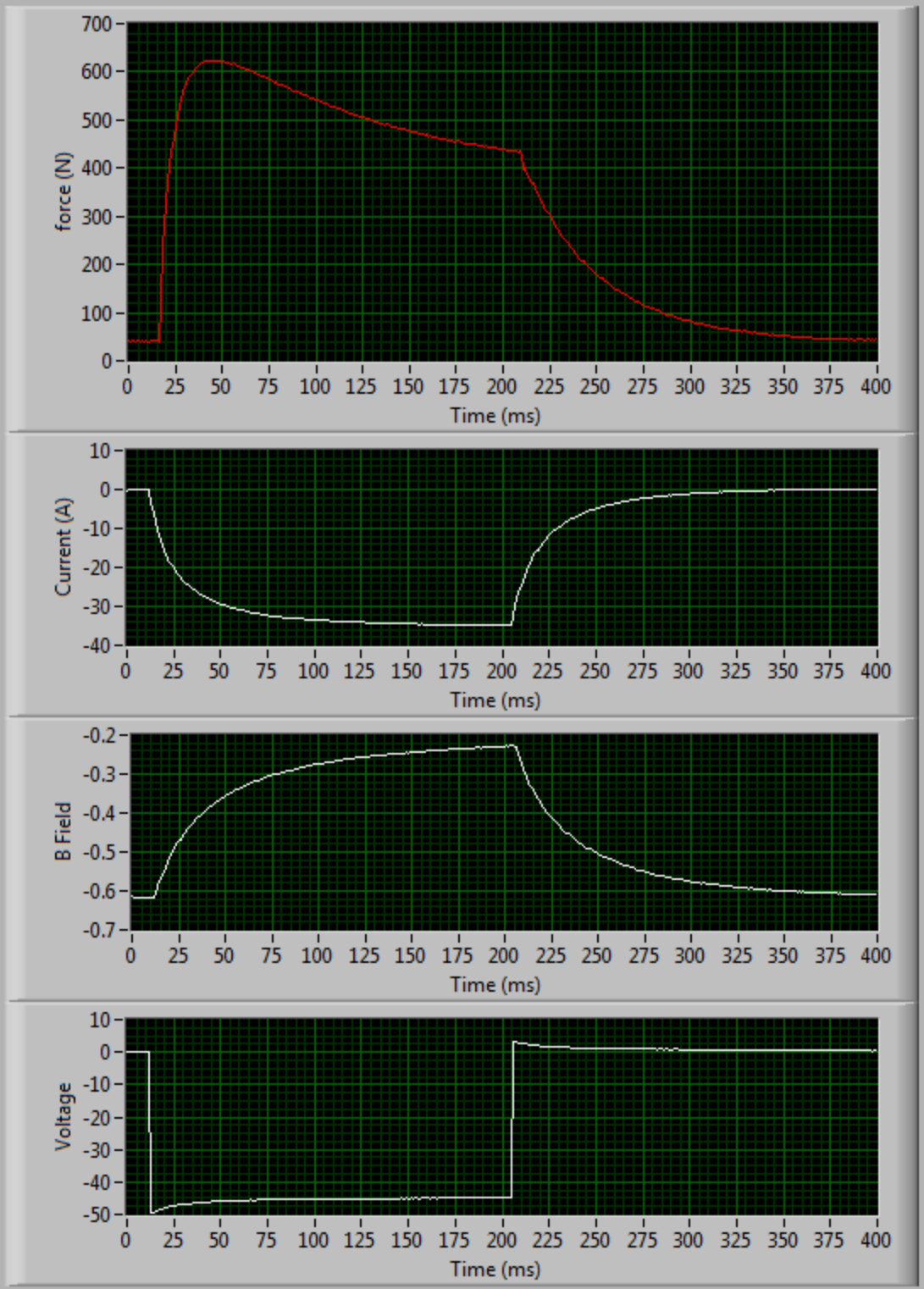

Figure 5.

Note that EMS can also determine the coil inductance and coil to coil mutual inductance. This inductance together with the coil resistance largely determines the coil electrical impedance transfer function. This transfer function accurately predicts the dynamic part of the signals shown in Figure 5.

Figure 6 shows an example of coil force (N), current (A), voltage (V) and magnetic flux density (T) recorded while a +35 A current pulse was applied to the coil (pushing).

Figure 6.

A comparison of these pulling and pushing data shows that there is a substantial difference in the absolute value of the forces generated. In the first experiment a current of -50 A produced a steady state force of -1800 N which equals 36 N/V. However in the second experiment a +35 A pulse produced only a +450 N force which equals approximately 13 N/V. Furthermore in the second experiment the force reaches an initial peak and then declines with time. This result cannot be predicted by the simple linear Lorentz force relation (Equation 1).
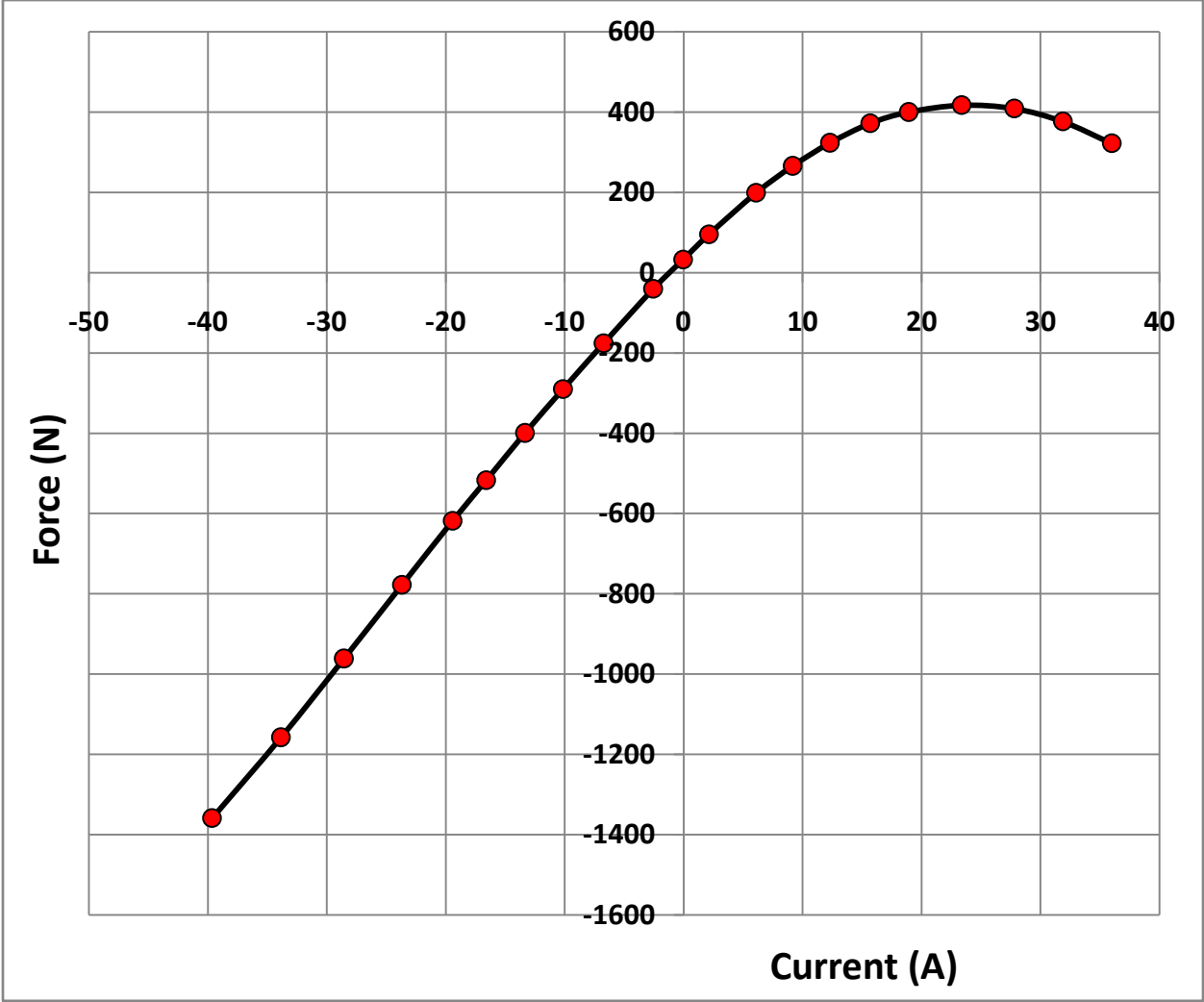
Figure 7. Actuator force shown as a function of coil current for both positive (push) and negative (pull) currents. Note the highly nonlinear response to positive currents.

Figure 7 clearly shows the highly nonlinear relation between coil positive current and force as measured in the second apparatus described above.

Finite Element Analysis

Finite element calculations require considerable computing resources. For this reason it is important to remove from the model any portions which are not likely to influence the calculations. In addition considerable time can be saved by taking a representative slab from the whole model. In our case we slice off the back and front of the actuator to leave a representative central slab which is 25 mm thick. If this slab contains 10% of the coil length (circumference) then any force calculation simply needs to be multiplied by 10 to get the predicted full coil force.

Figure 8.

Figure 8 shows a slab representing the iron path of the actuator (note that for simplicity we have squared off the rounded surfaces which would have resulted had we actually removed a slab from the middle of the actuator).

In Figures 9a and 9b the coil and magnets have been added. Note that the magnets have a gap on either side of them. This results in a more challenging geometry (as mentioned above) which further tests the predictive capability of EMS.
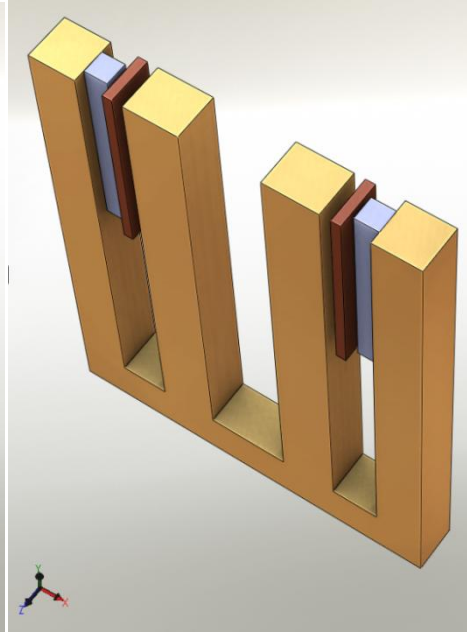
Figure 9a.   **Figure 9b.**

We need to model the air within our model. So this we simply create some extra SolidWorks parts to fill in any "air" space (see Figure 10) so that the entire volume containing our model is occupied. We also need to put some air around our model so that we can see the extent to which the magnetic field might extend beyond our linear actuator. The finite element algorithms also require that at the boundaries of our outer air the magnetic field intensity is near zero. The question arises as to how much outer air space should be added. The answer is that it is best to start by adding about 25% of the model x, y and z dimensions around the model as air. As seen below we can always check to see if the surrounding air is sufficient by inspecting the magnetic field intensity results.
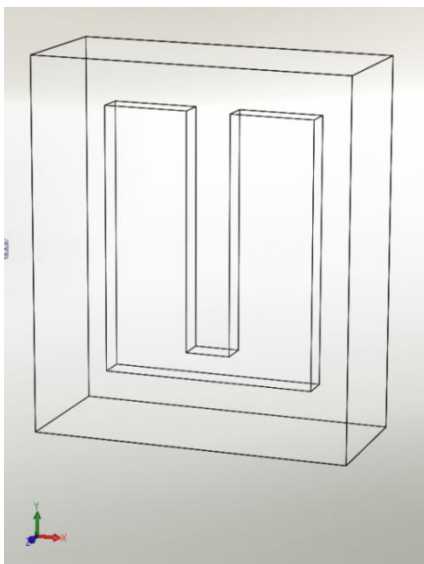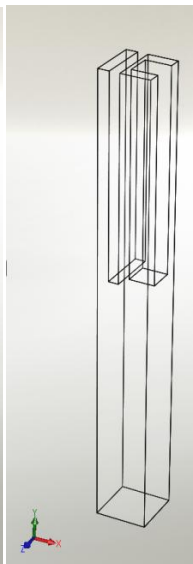

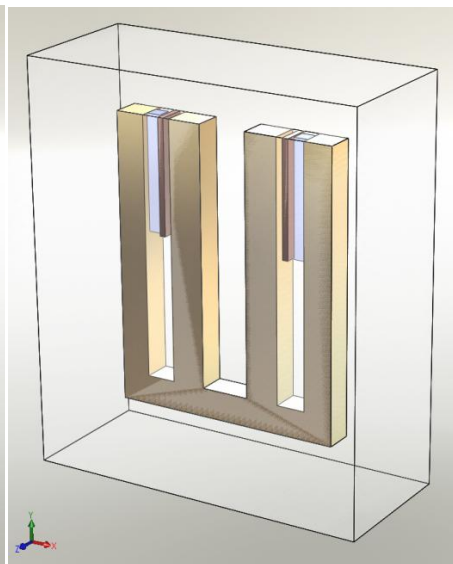**Figure 10a.**   **Figure 10b.**   **Figure 10c.**

Finally as a check that we do not have overlapping parts we perform a SolidWorks Interference check.

We now specify the Load/Restraint Normal Flux (see purple arrows Figure 11). We must also specify the magnitude and direction of the current flow in our coil (see arrows going into and out of the coil in Figure 11).
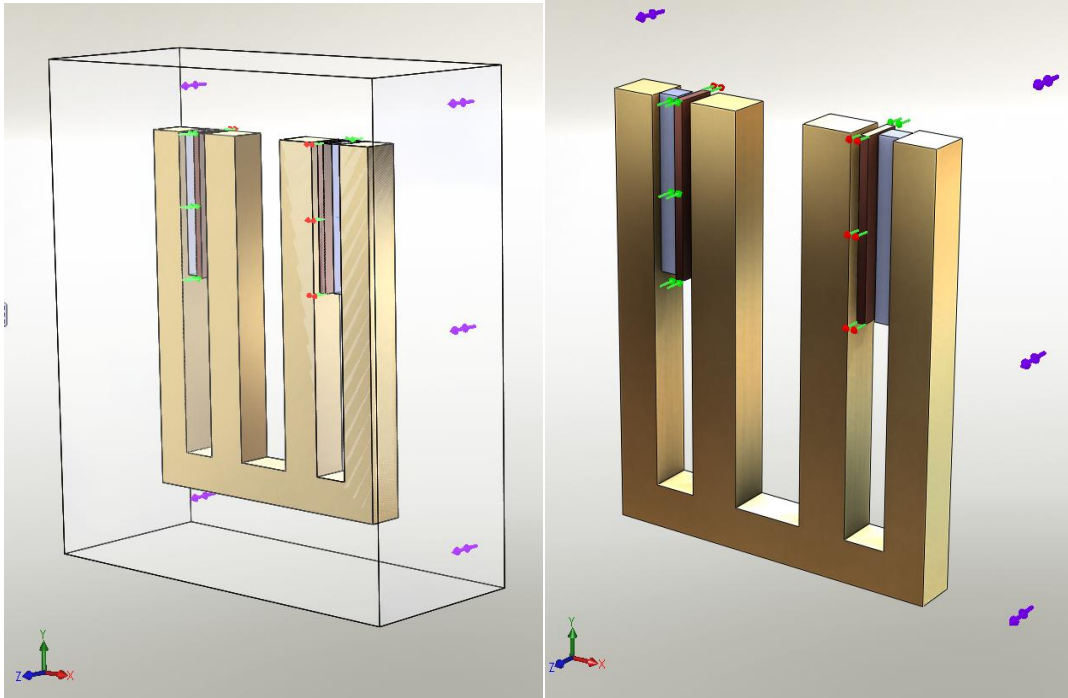

Figure 11a.   **Figure 11b.**

The magnetic orientation of each permanent magnet must be specified (see blue arrows in Figure 12).
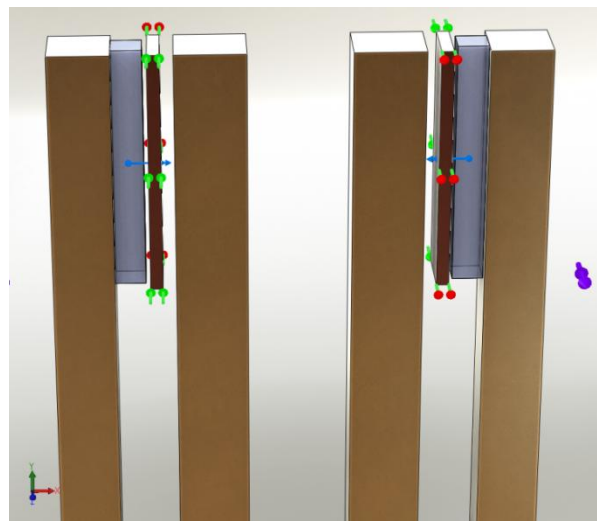
Figure 12.

As seen in Figure 13 the magnetic flux is set to run radially in from the permanent magnets across the first air gap and then through the coil and then through the inner air gap and then runs downs the inner iron path. It then runs radially out through the iron return and then up the outer iron path back to the magnets (see magnetic flux density plot below). The magnets used have an energy density of about 380 kJ/m^3.
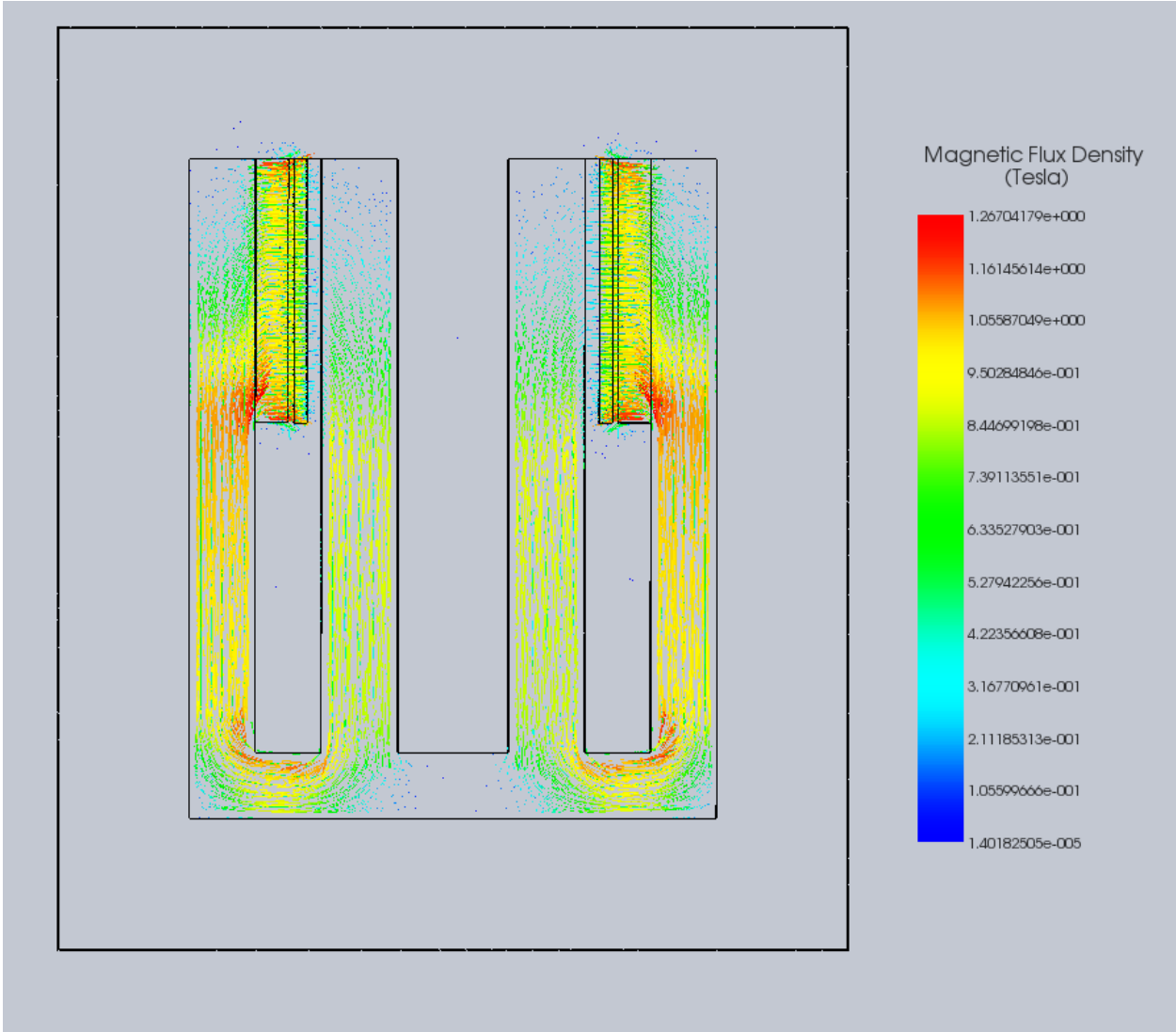

Figure 13. Static magnetic flux density as calculated by EMS when no current is flowing in the coil.

Finally we must provide EMS with a BH curve for the steel in our magnetic return path. The actual actuator uses 1018 steel (low carbon content). The BH curve for 1018 steel is shown in Figure 14.
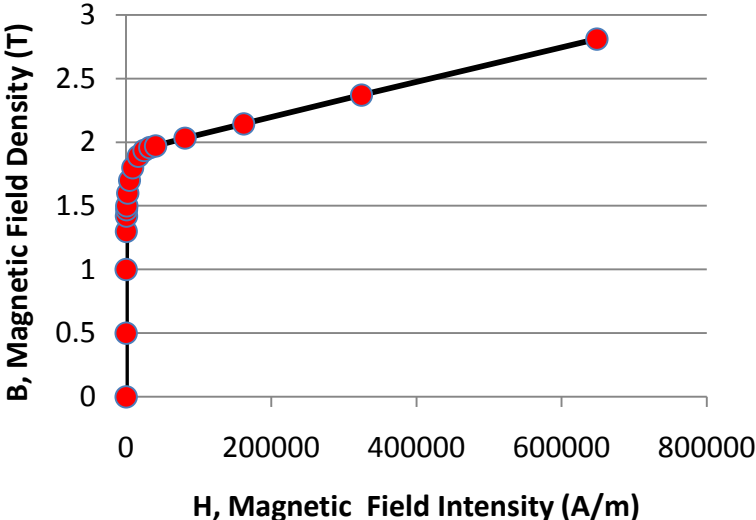

Figure 14. BH curve for 1018 low carbon content steel.

We also select suitable values for the mesh sizes for all the parts (see Figures 15a and b). Coarse meshes run faster but may give inaccurate results.
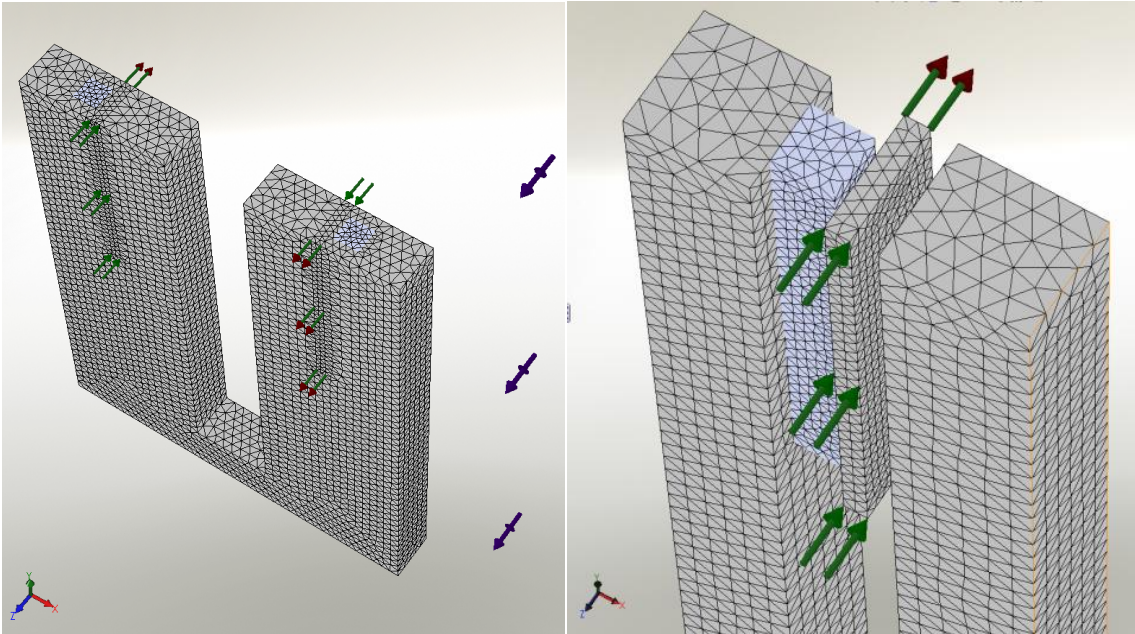

Figure 15a.   **Figure 15b.**

The number of mesh elements used in the analysis presented here was 667981 and the number of mesh nodes was 119393.

EMS Finite Element Analysis Results

Figure 16 shows the magnetic field intensity calculated by EMS. The magnetic field intensity is seen to be near zero (blue) at the outer boundaries of our surrounding air. Had the magnetic field intensity been significantly non zero at these outer boundaries the outer air surround part dimensions would have been increased.
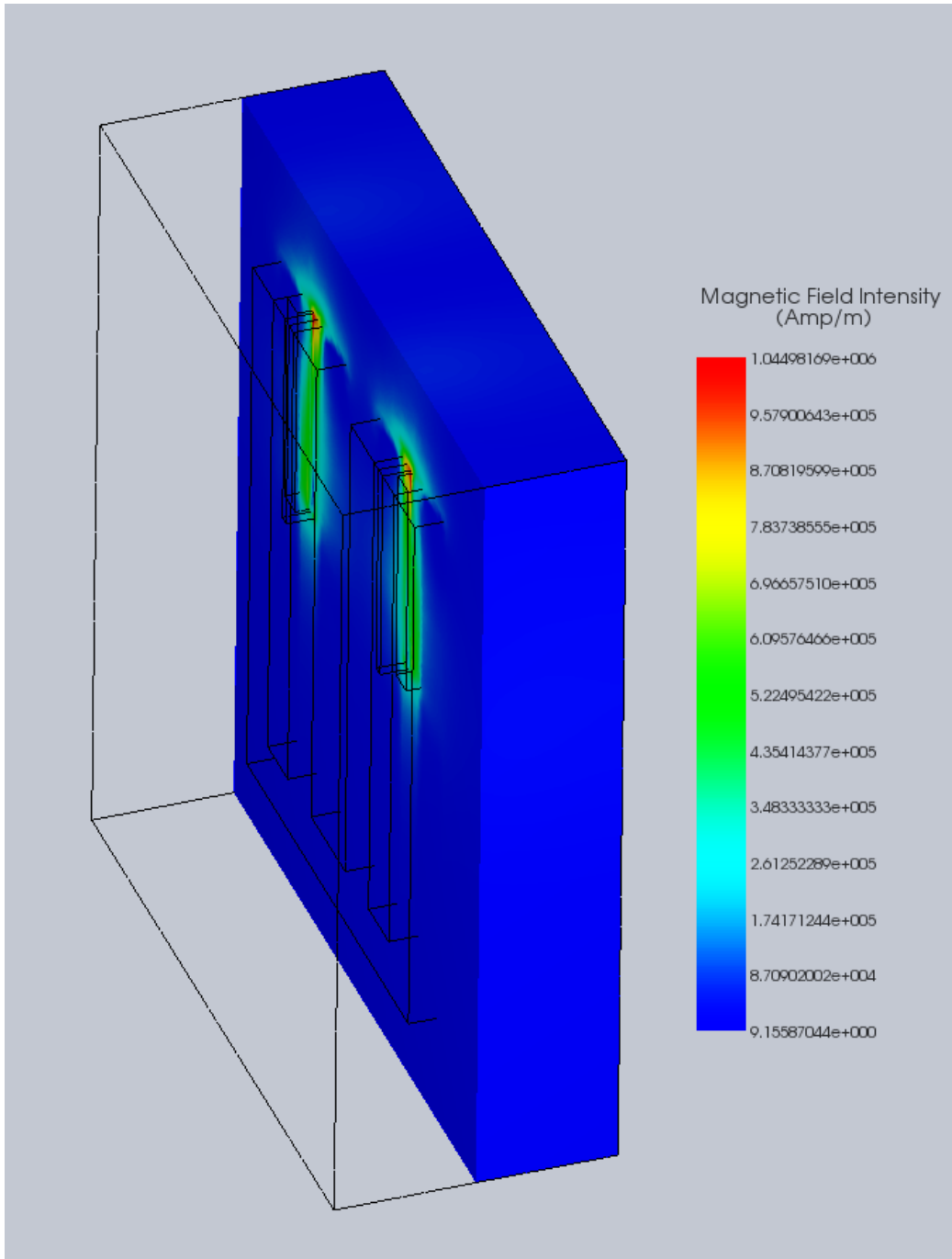

Figure 16

Figure 17 shows the current density as determined by EMS for a particular current flowing through the coil. In this case we were expecting a current density of 10^6 A/m^2 in our coil and indeed that is what is predicted (red).
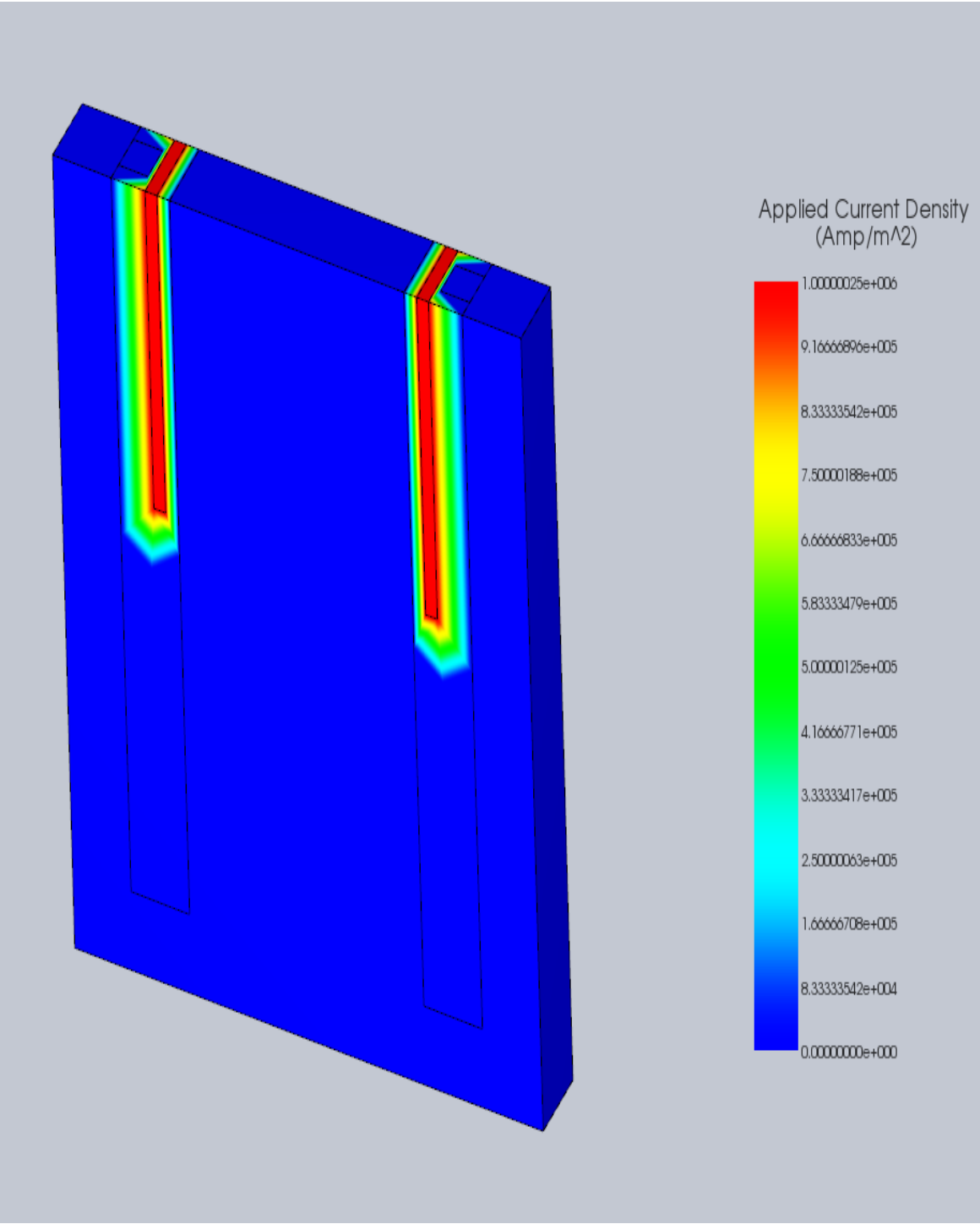

Figure 17.

With no current flowing in the coil we find that EMS predicts that the flux in the air gap ranges from about 0.7 T beside the magnet down to 0.3 T by the iron wall (see Figure 18). This is indeed what we measure experimentally.
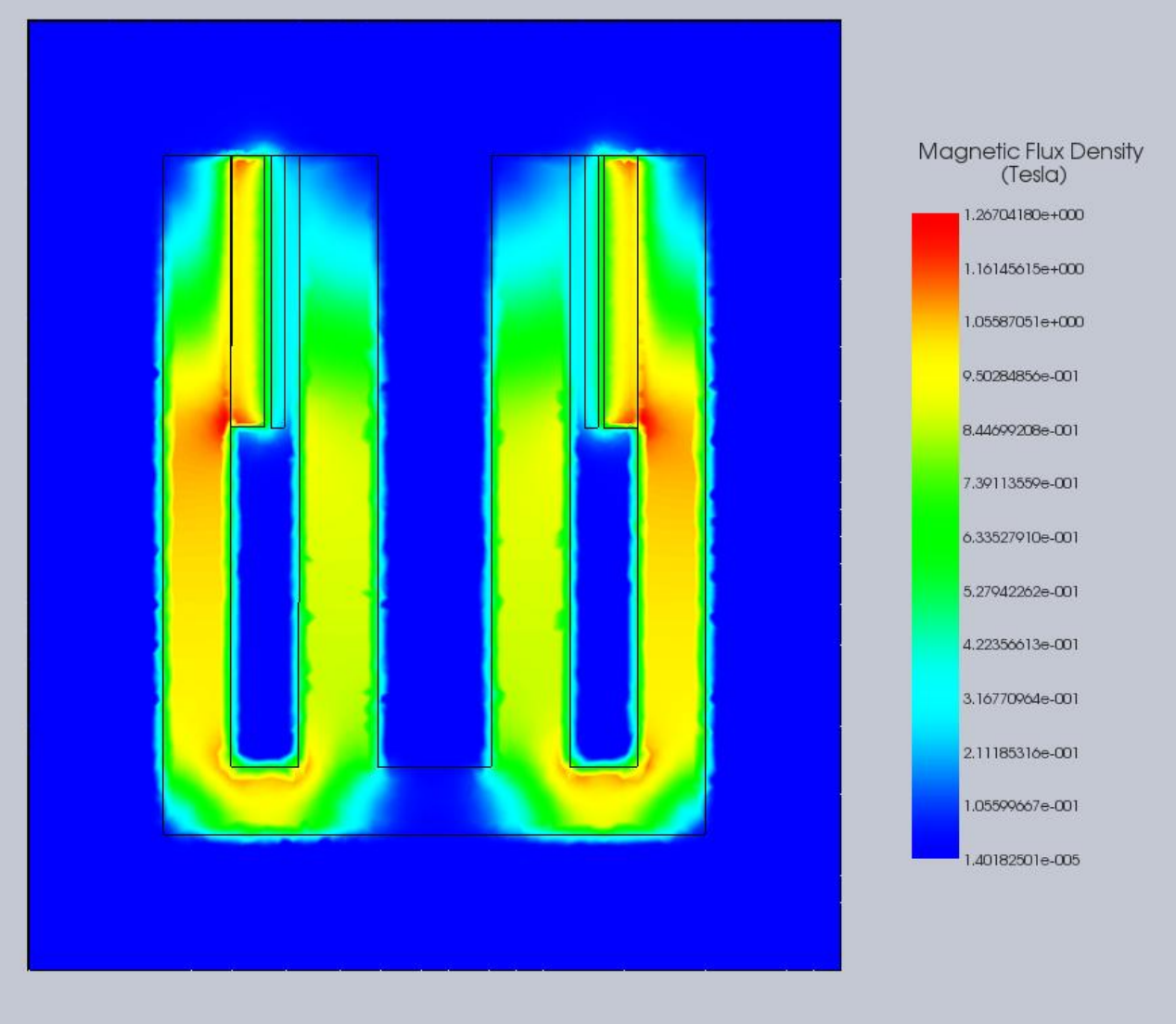

Figure 18

The magnetic flux density in the actuator as determined by EMS for a substantial current flowing in the coil is shown in Figure 19. Note the effect of the current flow on the magnetic flux (compare with the previous no coil current plot).
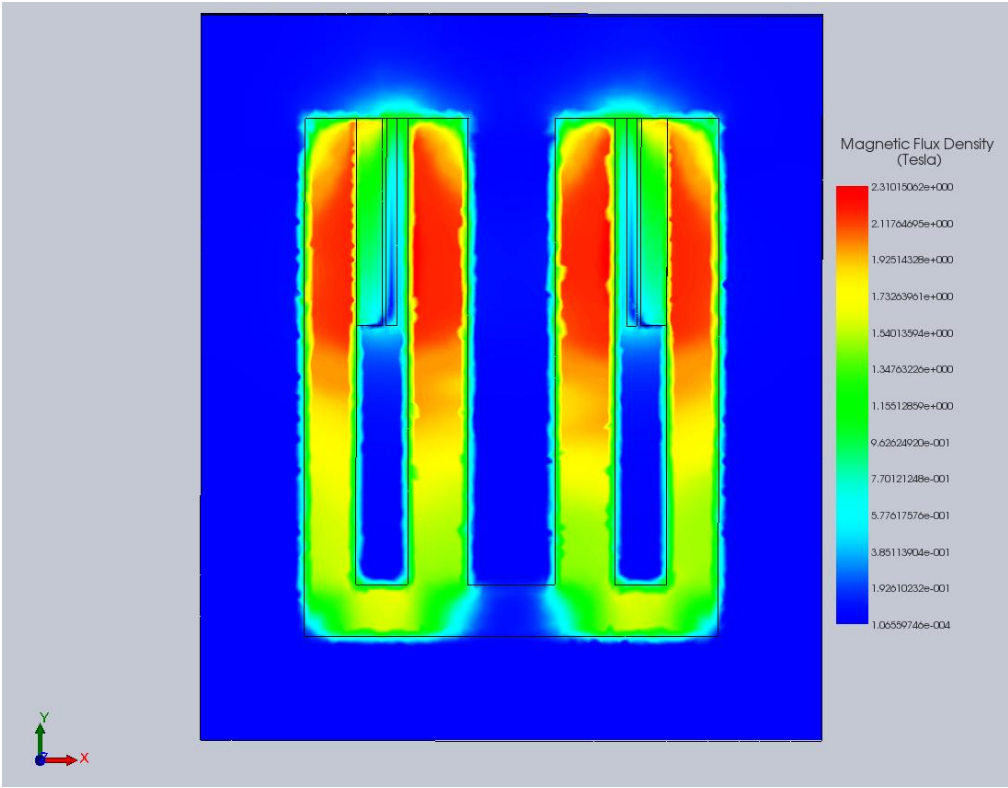

Figure 19.

Figure 20 shows the results of a series of EMS simulation in which the current flowing in the coil was varied from a large negative value to a large positive value. Note that the highly nonlinear positive current to force relation found experimentally is reproduced here.
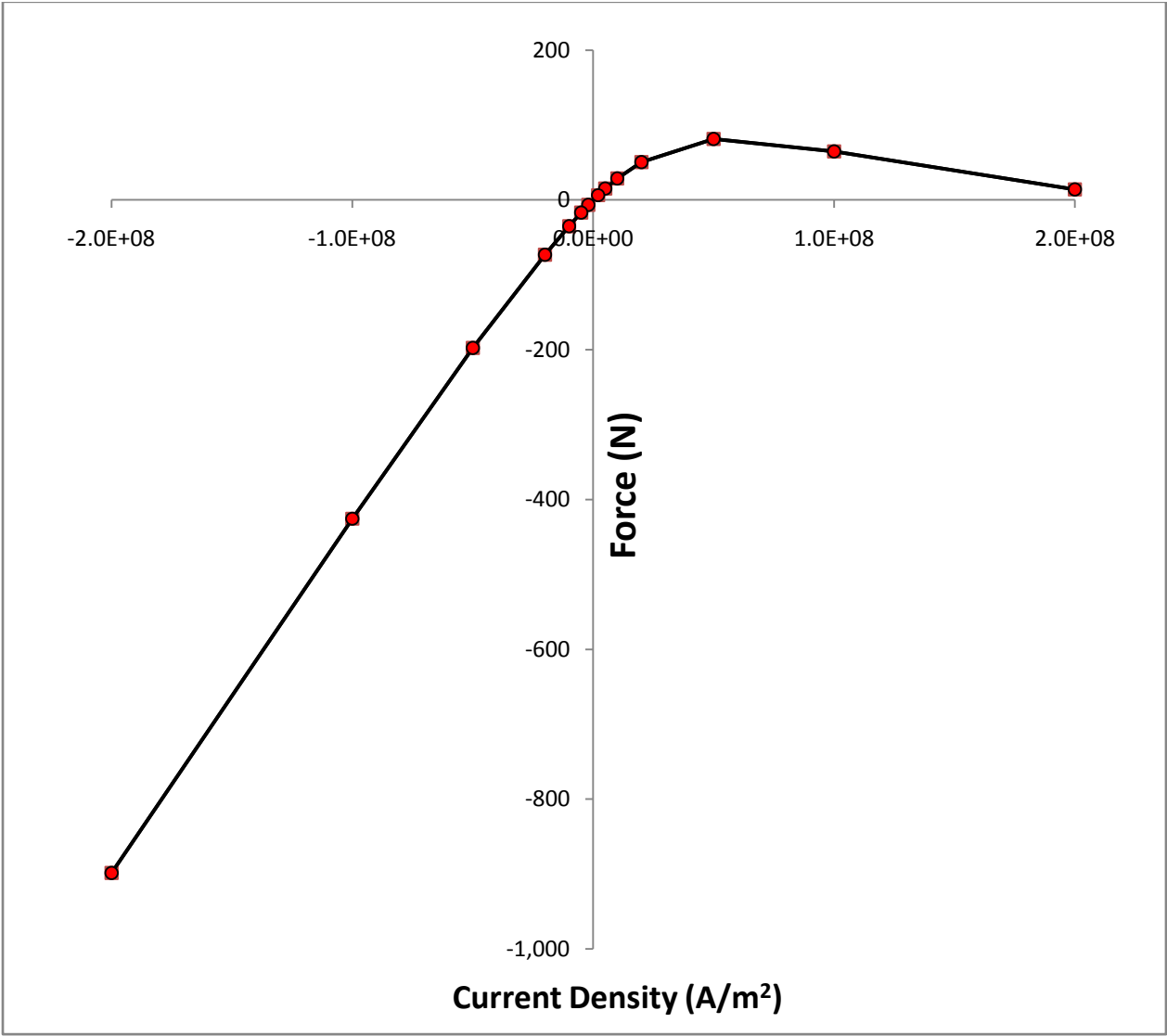

Figure 20.

Figure 21 shows the measured data plotted together with the EMS simulated data.
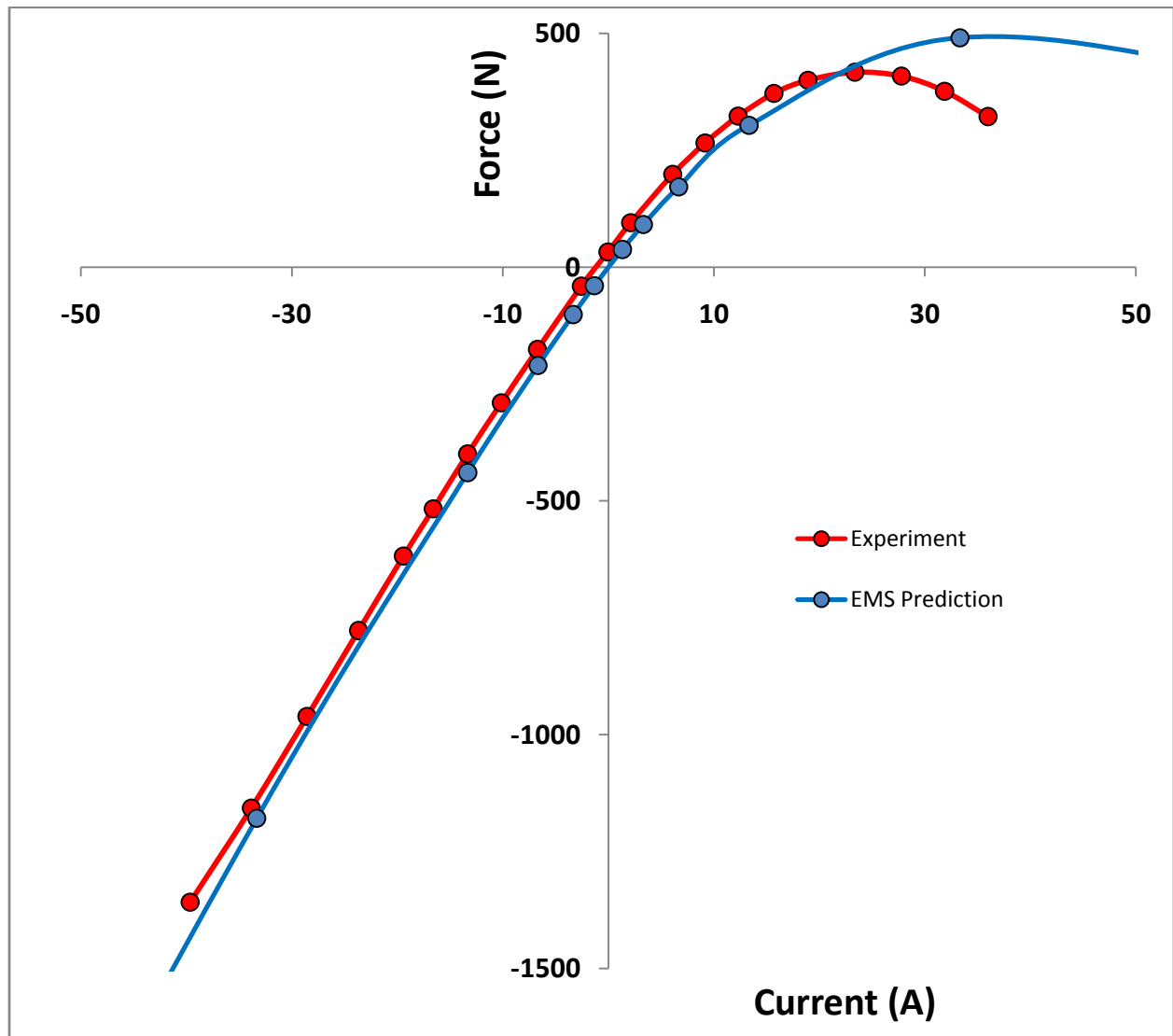

Figure 21.

Conclusions

A Lorentz force linear motion actuator was built to deliberately exhibit a highly nonlinear current for force relation even when the coil was completely immersed in the magnetic field. Magnets were arranged radially around the coil but only half the permissible number were included in order to generate a more complex actuator configuration to test the ability of the EMS electromagnetic finite element analysis software to handle more challenging magnetic path geometries. A detailed set of experiments were carried out on the actual actuator and a similar set of analyses were undertaken using the EMS magnetostatic electromagnetic finite element analysis software. EMS correctly accounted for the gross nonlinearities in the current to force measurements.

References

Taberner, A. J., Ball, N., Hogan, N.C., Hunter, I.W. **A portable Needle-free Jet Injector Based on a Custom High Power-Density Voice-coil Actuator.** *Proceedings of the 28th Annual International Conference of the IEEE EMBS, New York,* New York, USA, August 2006, 5001-5004.

Wendell, D., Hemond, B., Hogan, N.C., Taberner, A. J., Hunter, I.W. **The Effect of Jet Parameters on Jet Injection.** *Proceedings of the 28th Annual International Conf. of the IEEE EMBS*, New York, New York, USA, August 2006, 5005-5008.

Hemond, B., Wendell, D., Hogan, N.C., Taberner, A. J., Hunter, I.W. **A Lorentz-Force Actuated Autoloading Needle-Free Injector.** *Proceedings of the 28th Annual International Conference of the IEEE EMBS,* New York, New York, USA, August 2006, 679-682.